

**SUPPLEMENTARY MATERIALS FOR:**

**Mixing brine with oil triggered sphalerite deposition at Pine Point, Northwest Territories, Canada**

**Marko Szmihelsky<sup>1,2</sup>, Matthew Steele-MacInnis<sup>1</sup>, Wyatt M. Bain<sup>1</sup>, Hendrik Falck<sup>3</sup>, Robin Adair<sup>4</sup>, Brandon Campbell<sup>1</sup>, S. Andrew Dufrane<sup>1</sup>, Ashley Went<sup>1</sup> and Hilary J. Corlett<sup>5</sup>**

*<sup>1</sup>Department of Earth and Atmospheric Science, University of Alberta, 1-26 Earth Sciences Building, Edmonton, Alberta, T6G 2E3, Canada*

*<sup>2</sup>Department of Earth Sciences, Memorial University, 9 Arctic Avenue, St. John's, Newfoundland, A1B 3X5, Canada*

*<sup>3</sup>Northwest Territories Geological Survey, 4601 52 Ave, Yellowknife, Northwest Territories, X1A 1K3, Canada*

*<sup>4</sup>Osisko Metals Ltd., 1100 Avenue des Canadiens-de-Montréal (Bureau 300), Montréal, Québec, H3B 2S2, Canada*

*<sup>5</sup>Department of Physical Sciences, MacEwan University, Edmonton, Alberta, T5J 4S2, Canada*

**ADDITIONAL INFORMATION ON METHODS**

**Microthermometry of Fluid Inclusions**

Samples were prepared into doubly-polished sections with a thickness of 60  $\mu\text{m}$ . The sections were mounted using an ambient-temperature, acetone-soluble glue to avoid any heating of the samples prior to microscopy, so as to avoid any stretching of the contained fluid inclusions. Petrographic analyses were conducted using a custom-built Olympus BX53 microscope at the University of Alberta, equipped for transmitted light microscopy in the visible and near-infrared ranges, as well as reflected light and ultraviolet-light fluorescence.

Fluid inclusion microthermometry was conducted using a Linkam THGMS 600 heating-freezing stage mounted on the aforementioned Olympus BX53 microscope at the University of Alberta. Temperature of the stage was calibrated according to the triple point of  $\text{CO}_2$  ( $-56.6^\circ\text{C}$ ), the triple point of pure  $\text{H}_2\text{O}$  ( $0.0^\circ\text{C}$ ), and the critical point of pure  $\text{H}_2\text{O}$  ( $374.1^\circ\text{C}$ ) using synthetic fluid inclusion standards.

Primary and pseudo-secondary fluid-inclusion assemblages were identified according to the criteria outlined by Roedder (1984). Specifically, assemblages were deemed primary when they occurred along well-defined growth zones, whereas pseudo-secondary assemblage were those that occurred along cross-cutting trails that were truncated by later growth zones.

Because the brine inclusions analyzed here had very low volume fractions of vapor at ambient temperature (Fig. 2), we were cautious to avoid artificially high homogenization temperatures resulting from accidental stretching (Roedder, 1984). Therefore, during microthermometry, the samples were first heated to measure the homogenization temperatures, prior to freeing to measure the melting temperatures.

Whenever possible, we used the combination of ice-melting and hydrohalite-melting temperatures in an inclusion to estimate both total salinity and Ca:Na ratio the model system  $\text{H}_2\text{O}$ - $\text{NaCl}$ - $\text{CaCl}_2$  (Steele-MacInnis et al., 2011). In cases where only one or the other melting

temperature was observed, we estimated salinity in terms of equivalent weight percent NaCl (Steele-MacInnis et al., 2012).

#### **Laser Raman spectroscopy**

Raman analyses were conducted at MacEwan University using a Bruker SENTERRA spectrometer and a 532 nm Ar<sup>+</sup> laser, focused to a 1 µm spot through a 100x objective mounted on a standard petrographic microscope. All spectra were acquired on unoriented grains using a laser power of 20 mW and two to three, 5-20s exposures summed to the final reported spectra. Baseline subtraction and background reduction were applied using the Fityk™ software packages. Spectra were interpreted using the RRUFF database (Lafuente et al., 2016; mineral species), Frezzotti et al. (2012; hydrocarbons), and Walter et al. (2016; Brine sulfate).

#### **Laser ablation inductively coupled plasma mass spectrometry**

The elemental composition of the fluid inclusions was analyzed at the Canadian Center for Isotopic Microanalysis at the University of Alberta using a Thermo Scientific ICAP-Q quadrupole inductively coupled plasma mass spectrometer (ICP-MS) coupled with a New Wave UP-213 laser ablation system. Helium (0.5 L/min) gas transported ablated particles from the ablation cell to the argon plasma. The laser operated at 10 Hz and 70% power. Beam diameter was adjusted as needed to fully ablate the fluid inclusions, between 25 µm and 65 µm. In sphalerite crystals that showed poorer coupling with the laser (particularly, light-colored to colorless sphalerite), we set the laser to 20 Hz and 80% power to improve ablation. We used both

the NIST 610 and NIST 612 reference materials as external standards to calibrate sensitivity and drift.

The ICP-MS was set to detect 18 elements:  $^{43}\text{Ca}$ ,  $^{23}\text{Na}$ ,  $^{39}\text{K}$ ,  $^{24}\text{Mg}$ ,  $^{137}\text{Ba}$ ,  $^{88}\text{Sr}$ ,  $^{208}\text{Pb}$ ,  $^{57}\text{Fe}$ ,  $^{55}\text{Mn}$ ,  $^7\text{Li}$ ,  $^{85}\text{Rb}$ ,  $^{133}\text{Cs}$ ,  $^{63}\text{Cu}$ ,  $^{68}\text{Zn}$ ,  $^{73}\text{Ge}$ ,  $^{111}\text{Cd}$ ,  $^{115}\text{In}$  and  $^{75}\text{As}$ , all at a dwell time of 10 ms. Of the elements analyzed, Na, K, Mg, Ca, Sr, Rb, Ba, and Pb were detected in the inclusions; all other elements were either below their respective detection limits, or masked by the sphalerite matrix (particularly Zn and Fe). The LA-ICP-MS data were reduced using the SILLS software package (Guillong et al., 2008). The internal standard for the brine inclusions was either equivalent weight percent NaCl (for inclusions in which only ice melting was observed), or the estimated “true” NaCl concentration in terms of  $\text{H}_2\text{O}$ -NaCl- $\text{CaCl}_2$  (for inclusions in which both ice and hydrohalite melting were observed; Schlegel et al., 2012; Steele-MacInnis et al., 2016). The internal standard for the Oil inclusions was an estimated Na concentration of 100 ppm, based on a survey of ICP-OES analyses of various crude oils (de Oliveira Souza et al., 2015). The Na concentrations of natural crude oils show little variability, generally on the order of ~10 to <200 ppm (Wauquier, 1998). The calculated concentrations of metals in the oil inclusions will scale proportionally to estimated Na concentration as internal standard. For example, if the specified Na concentration of the oil is reduced by 50%, then the calculated Pb concentrations will be similarly reduced by 50%. Based on available analytical data for Na concentrations of crude oils (de Oliveira Souza et al., 2015), a value of 100 ppm was selected as a conservative estimate, and the true Pb concentrations are expected to fall within the range of 0.1 to 2x the reported values based on this internal standard.

90

91 **DATA REPOSITORY REFERENCES CITED**

92

93 de Oliveira Souza, M., Ribeiro, M.A., Carneiro, M.T.W.D., Athayde, G.P.B., de Castro, E.V.R.,

94 da Silva, F.L.F., Mathos, W.O., and de Queiroz Ferreira, R., 2015, Evaluation and

95 Determination of Chloride in Crude Oil Based on the Counterions N, Ca, Mg, Sr, and Fe,

96 Quantified by ICP-OES in the Crude Oil Brine Extract: Fuel, v. 154, p. 181–187.

97 Frezzotti M. L., Tecce F., and Casagli A., 2012, Raman spectroscopy for fluid inclusion analysis.

98 Journal of Geochemical Exploration, v. 112, p. 1–20.

99 Guillong, M., Meier, D.L., Allan, M.M., Heinrich, C.A., and Yardley, B.W.D., 2008, Appendix

100 A6: SILLS: A MATLAB-Based Program for the Reduction of Laser Ablation ICP-MS Data

101 of Homogenous Materials and Inclusions: Mineralogical Association of Canada Short

102 Course 40, p. 328–333, <http://www.igmr.ethz.ch/research/fluids/software>. (accessed July

103 2020).

104 Lafuente, B., Downs, R. T., Yang, H. & Stone, N., 2016, The power of databases: The RRUFF

105 project: Highlights in Mineralogical Crystallography, p. 1-29.

106 Roedder, E., 1984, Fluid inclusions: Reviews in Mineralogy, v. 12, 646 p.,

107 doi:10.1515/9781501508271.

108 Schlegel, T.U., Wälle, M., Steele-MacInnis, M., and Heinrich, C.A., 2012, Accurate and precise

109 quantification of major and trace element compositions of calcic-sodic brines in fluid

110 inclusions by combining microthermometry and LA-ICPMS analysis. Chemical Geology, v.

111 334, p. 144-153. doi:10.1016/j.chemgeo.2012.10.001

112 Steele-MacInnis, M., Lecumberri-Sanchez, P., and Bodnar, R.J., 2012, HokieFlincs\_H2O-NaCl :

113 A Microsoft Excel spreadsheet for interpreting microthermometric data from fluid

inclusions based on the PVTX properties of H<sub>2</sub>O–NaCl: Computers & Geosciences, v. 49,  
p. 334–337, doi:10.1016/j.cageo.2012.01.022.

Steele-MacInnis, M., Ridley, J., Lecumberri-Sanchez, P., Schlegel, T., and Heinrich, C.A.,  
2016, Application of low-temperature microthermometric data for interpreting  
multicomponent fluid inclusion compositions. Earth-Science Reviews, v. 159, p. 14-35.  
doi:10.1016/j.earscirev.2016.04.011

Walter, B., Steele-MacInnis, M., and Markl, G., 2017, Sulfate brines in fluid inclusions of  
hydrothermal veins: Compositional determinations in the system H<sub>2</sub>O-Na-Ca-Cl-SO<sub>4</sub>.  
Geochimica et Cosmochimica Acta, v. 209, p. 184-203. doi:10.1016/j.gca.2017.04.027

Wauquier, J.-P., 1998, Petroleum Refining, Volume 2, Separation Processes. Editions Technip,  
Paris, 704 pp.

128     **DATA REPOSITORY TABLES**

129  
130     Table DR1: Samples and sample locations.

Sample Number	Location	Description
002.1	N38 (Main Trend)	Coarse sphalerite grown into open space filled by late-stage calcite.
006.3	L37 (Main Trend)	Series of cross-cutting “blue-vein” dolomite veins wherein coarse sphalerite postdates the “blue-vein” dolomite in each successive vein.
007	L37 (Main Trend)	Sphalerite plus dolomite grown into open space filled by late-stage calcite.
011.1	K77 (Main Trend)	“Blue-vein” dolomite vein containing coarse galena and sphalerite plus late-stage calcite.
22A2	N38 (Main Trend)	Breccia with incorporated fragments of carbonate wall rock and earlier-formed (now brecciated) fragments of coarse sphalerite.
22B2	N38 (Main Trend)	Breccia with incorporated fragments of carbonate wall rock and earlier-formed (now brecciated) fragments of coarse sphalerite.

131  
132

Inclusion Number	Inclusion Type	T <sub>H</sub> (°C)	T <sub>M Ice</sub> (°C)	Salinity (eq. wt% NaCl)
1	Brine	59.7	-39.7	35.9
2	Brine	93.7	-26.6	26.6
3	Brine	97.9	-34.3	31.5
4	Brine	115.6	-33.9	31.2
5	Brine	114.6	-38.8	34.3
6	Brine	96.7	-38.0	35.1
7	Brine	96.7	-43.8	40.0
8	Brine	100.7	-43.8	40.0
9	Brine	86.8	-34.0	31.3
10	Brine	86.8	-34.0	31.3
11	Brine	90.3	-21.7	34.1
12	Brine	79.4	-38.0	36.4
13	Brine	79.7	-34.9	34.3
14	Brine	79.7	-34.9	34.3
15	Brine	80.9	-35.7	35.0
16	Brine	79.4	-38.0	36.4
17	Brine	100.4	-38.8	35.0
18	Brine	91.4	-40.1	36.4
19	Brine	91.4	-40.1	36.3
20	Brine	100.9	-40.3	36.4
21	Brine	94.6	-32.6	30.3
22	Brine	63.4	-19.6	22.1



Inclusion Number	Inclusion Type	T <sub>H</sub> (°C)	T <sub>M</sub> (°C)*
23	Oil	71.8	-
24	Oil	70.1	-
25	Oil	77.3	-
26	Oil	101.8	-
27	Oil	101.9	-
28	Oil	82.3	-
29	Oil	66.8	-
30	Oil	71.3	-
31	Oil	81.3	-
32	Oil	66.3	-
33	Oil	51.4	-
34	Oil	53.2	-
35	Oil	49.8	-
36	Oil	52.6	-
37	Oil	52	-
38	Oil	56.9	-
39	Oil	71.3	-
40	Oil	66.2	-
41	Oil	72.6	-
42	Oil	73.4	-
43	Oil	69.8	-
44	Oil	74.8	-

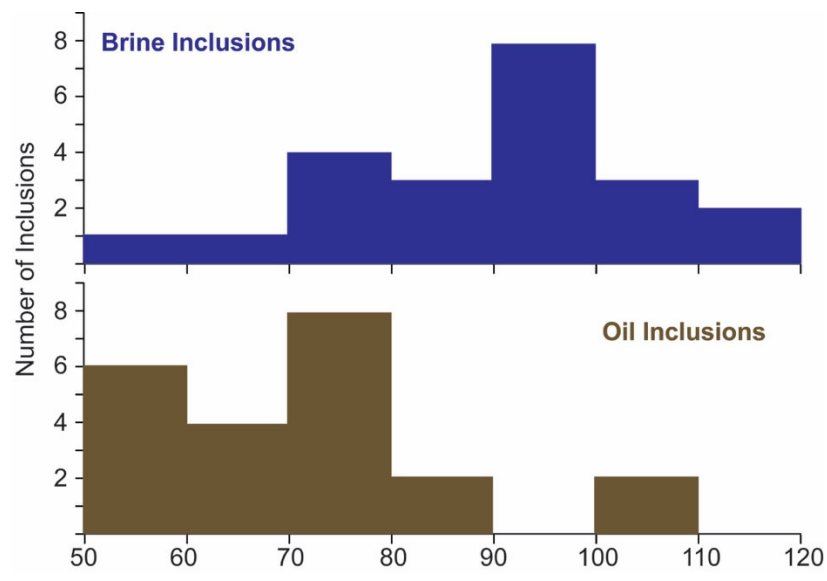
\*Oil inclusions did not freeze.

Inc. Number	Inc. Type	Na (ppm)	Mg (ppm)	K (ppm)	Ca (ppm)	Mn (ppm)	Cu (ppm)	Ge (ppm)	Rb (ppm)	Sr (ppm)	Ba (ppm)	Pb (ppm)
1	Brine	42885.2	11939.6	4694.7	62899.7	<0.7	12.1	404.3	11.6	1536.8	25.2	<0.009
2	Brine	31709.6	9201.6	3982.1	45745.8	36.9	48.0	41.4	11.7	1156.7	28.1	336.3
3	Brine	30751.3	11735.8	18414.6	51955.7	<0.7	29.6	107.4	17.1	1163.0	21.8	333.1
4	Brine	31808.2	10430.7	11862.2	55469.0	<8.0	<2.5	30.2	9.0	1219.8	11.7	318.2
5	Brine	41277.0	11481.2	17451.5	55911.8	48.5	6.1	<3.7	10.1	1283.1	19.6	62.2
6	Brine	46303.1	12988.0	20242.0	64160.2	20.7	3.9	211.7	10.4	1530.3	17.7	564.4
7	Brine	48308.1	13598.1	18797.4	62180.5	<8.7	<2.5	31.8	21.0	1528.8	19.6	392.0
8	Brine	26877.5	8798.9	4852.2	95790.2	159.3	<2.9	299.2	2.7	1987.9	20.1	116.2
9	Brine	35535.1	9114.1	11241.8	55079.8	<17.2	362.9	26.8	5.0	1390.8	24.4	299.7
10	Brine	38083.4	10884.0	11185.4	50040.1	<2.1	<0.5	<0.7	12.9	1235.0	22.7	<0.03
11	Brine	37429.4	10908.8	8191.8	61591.8	26.7	587.2	55.8	4.3	1404.7	19.1	191.7
12	Brine	41904.1	11805.1	7566.5	64263.4	8.5	243.4	<0.2	7.7	1548.4	19.6	129.2
13	Brine	41815.0	11167.1	6893.4	58435.5	<1.8	203.2	<0.3	8.1	1475.1	25.5	<0.02
14	Brine	32426.6	9472.9	5614.6	70139.1	74.3	160.4	<0.3	5.6	1325.8	19.0	<0.02
15	Brine	44844.1	11423.8	8425.8	57210.2	90.9	<0.3	58.2	16.3	1438.3	16.2	486.0
16	Brine	43241.8	12741.0	8230.3	61268.0	59.9	45.7	30.4	7.6	1482.4	22.1	<0.02
17	Brine	27007.8	49543.6	4300.8	12493.5	91.3	<0.3	<0.4	41.0	<0.02	523.4	96.1
18	Brine	17774.9	39224.5	29843.6	27215.6	246.7	<0.9	256.5	8.0	5219.1	179.1	2711.6
19	Brine	14924.9	38092.6	30680.2	30706.3	1248.5	2183.7	5328.0	176.6	4193.0	16.7	900.7
20	Brine	15648.3	30998.7	21457.8	47560.1	229.0	<1.6	<2.2	60.9	3396.1	191.3	<0.1
21	Brine	32997.4	10514.0	6378.8	54020.8	<4.9	<1.2	288.1	33.9	1378.9	10.7	190.0
22	Brine	25926.5	9601.4	6053.6	33873.4	<3.5	13.0	<1.1	<0.4	968.7	12.4	<0.07

Table DR4, Continued

Inc. Number	Inc. Type	Na (ppm)	Mg (ppm)	K (ppm)	Ca (ppm)	Mn (ppm)	Cu (ppm)	Ge (ppm)	Rb (ppm)	Sr (ppm)	Ba (ppm)	Pb (ppm)
23	Oil	100.0	34.2	9.2	199.7	<0.7	0.4	<0.3	<0.1	1.2	<0.05	<0.02
24	Oil	100.0	27.7	13.6	163.1	<0.3	<0.1	<0.1	<0.03	3.9	0.05	0.9
25	Oil	100.0	28.9	<7.9	<304.7	<1.8	<0.4	1.5	<0.2	4.0	<0.01	<0.04
26	Oil	100.0	19.6	13.8	<204.6	<1.2	<0.3	1.5	<0.1	2.6	0.1	<0.02
27	Oil	100.0	19.2	17.4	201.3	<0.9	<0.2	<0.2	<0.1	2.1	<0.1	1.5
28	Oil	100.0	19.8	5.4	<173.7	<1.0	<0.2	<0.5	<0.1	2.4	<0.1	<0.02
29	Oil	100.0	26.2	6.9	<189.2	<1.1	<0.3	0.9	<0.1	4.1	<0.1	<0.02
30	Oil	100.0	13.9	17.5	267.4	<1.5	<0.3	<0.5	<0.1	3.0	<0.1	<0.03
31	Oil	100.0	6.8	6.4	392.1	<0.9	<0.2	<0.3	<0.1	4.3	0.1	<0.02
32	Oil	100.0	23.6	15.4	<141.7	<0.8	<0.2	<0.3	<0.04	3.7	0.04	<0.02
33	Oil	100.0	35.4	19.3	304.2	<0.5	<0.1	<0.1	<0.2	2.9	0.1	<0.01
34	Oil	100.0	27.1	<14.2	<494.7	<2.9	<0.7	1.5	<0.2	3.9	0.1	5.2
35	Oil	100.0	25.7	14.6	94.8	<0.3	<0.1	0.6	<0.02	3.2	0.04	0.5
36	Oil	100.0	43.4	15.0	191.2	<0.7	<0.1	<0.3	<0.1	4.3	0.1	0.01
37	Oil	100.0	71.8	71.3	3380.1	23.0	<0.9	16.6	2.5	11.2	0.7	17.8
38	Oil	100.0	<1.3	<30.1	1871.0	11.7	0.2	5.2	<0.1	<0.1	<0.1	<0.1
39	Oil	100.0	28.9	11.0	132.7	0.3	<0.1	<0.7	<0.02	3.1	0.1	0.2
40	Oil	100.0	26.0	<6.4	<227.8	<1.3	<0.3	<0.6	0.1	3.5	0.1	<0.02
41	Oil	100.0	53.6	<29.1	<1032.5	<6.0	<1.4	<2.1	<0.5	7.9	<0.4	0.2
42	Oil	100.0	27.2	11.5	101.2	<0.3	<0.1	<0.1	<0.03	3.3	0.04	0.3
43	Oil	100.0	24.4	14.9	<114.6	<0.7	<0.2	<0.2	<0.05	3.4	0.04	<0.01
44	Oil	100.0	24.0	14.6	119.5	<0.6	0.2	<0.1	<0.04	2.9	0.1	<0.01

154 DATA REPOSITORY FIGURES



155  
156  
157 Figure DR1. Histograms of homogenization temperatures of brine (top) and oil (bottom)  
158 inclusions.